PHYSICAL REVIEW A VOLUME 58, NUMBER 1 JULY 1998

Population trapping and laser-induced continuum structure in helium: Experiment and theory

T. Halfmann, L. P. Yatsenko,* M. Shapiro,† B. W. Shore,‡ and K. Bergmann
Fachbereich Physik der Universität, 67653 Kaiserslautern, Germany
(Received 25 March 1998)

We report the observation of laser-induced structure (LICS) in the flat photoionization continuum of helium. The structure is a strong and spectrally sharp resonance, showing both enhanced and diminished ionization (a Beutler-Fano profile). Our observations show, in an otherwise unstructured continuum, pronounced ionization suppression (as much as 70%), which is due to population trapping associated with LICS. We also show the effect of dynamic Stark shifts upon the LICS profile. A discussed theoretical model, incorporating significant dynamic Stark shifts, gives a quantitatively accurate description of the line profile for a wide range of pulse intensities. [S1050-2947(98)51807-0]

PACS number(s): 42.50.Hz, 32.80.Fb, 32.80.Qk

INTRODUCTION

In recent years our understanding of how laser fields interact with a continuum of energy levels has progressed substantially. The continuum is no longer viewed merely as a dissipative environment that is best described by a set of kinetic equations (often using approximations such as the Fermi golden rule). Theoretical and experimental work [1–7] has shown that laser fields may often maintain perfect coherence involving continuum states. In particular, laser interactions with a continuum have been shown to exhibit Rabi-type oscillations [4] and to lead to essentially complete population transfer to and from a continuum. In theory, a continuum can serve as an intermediary for a stimulated Raman adiabatic passage (STIRAP) process in which nearly complete population transfer occurs between two bound states [6,8–10]. In practice, however, this is a much more difficult task [6,8] than STIRAP, which involves bound intermediate states [11].

It has long been recognized that autoionization line profiles reveal the effect of interference between two ionization channels [12,13]. Destructive interference may lead to complete suppression of photoionization at a specific wavelength. One of the more interesting coherent phenomena involving a continuum is revealed by using a laser field to embed a bound-state resonance into a possibly otherwise featureless continuum. Such ''laser-induced continuum structure'' (LICS) [1,14–16] can be detected, among other possibilities, by a second (weaker) laser field that induces a transition from a populated bound state to the previously unstructured continuum. Observations of LICS of photoionization near autoionization resonances have been reported [2,19]. Under appropriate conditions the presence of the strong laser field (which alone produces no ionization) can suppress the photoionization of a probe laser; the two fields create a coherent-superposition state that is immune to photoionization (a trapped state [17,18]). Ionization enhancement is the dominant feature, in previously observed LICS in photoionization, of an otherwise *unstructured* continuum [20–22], with some suppression (a few percent) also recognizable. Here we present experimental data, with theoretical substantiation, for substantial (70%) ionization suppression and population trapping. The nearly complete suppression of photoionization revealed by our data indicates quite clearly the presence of strong coherent interaction mediated by the photoionization continuum.

We also demonstrate, both experimentally and theoretically, how dynamic Stark shifts alter the LICS structures (inducing shifts and widths). The high spectral resolution achieved in this experiment renders this LICS a spectroscopic tool for revealing coherence properties of the photoionization continuum and measuring laser-induced Stark shifts. We find excellent agreement between experiment and a simple model-potential calculation (no adjustable parameters) of atomic parameters, including continuum properties.

EXPERIMENT

A pulsed beam of helium is expanded through a nozzle (general valve; opening diameter 0.8 mm) with a stagnation pressure of 1200 mbar. The atoms are excited from the ground state $1s\,^1S_0$ to the metastable singlet state $2s\,^1S_0$ by electron impact in a gas discharge that is operated 4 mm behind the nozzle. A skimmer (diameter 0.8 mm) is placed 40 mm away from the nozzle to collimate the atomic beam and to separate the source chamber from the region of interaction and detection.

To detect helium ions mass selectively, we use a double-thickness microsphere plate (El Mul Technologies) and a short time-of-flight segment. The output current of the microsphere plate is amplified with fast broadband amplifiers and is integrated in a boxcar gated integrator (EG&G 4121 B).

Figure 1 shows a schematic diagram of the states and transitions involved in our experiment. A dressing pulse couples the (initially unpopulated) excited state $4s\,^1S_0$ to the ionization continuum thereby inducing the continuum structure. This is probed by a weaker laser pulse that couples the

*Permanent address: Institute of Physics, Ukrainian Academy of Sciences, Prospekt Nauki 46, Kiev-22, 252650, Ukraine.

†Permanent address: Department of Chemical Physics, The Weizmann Institute of Science, Rehovot, Israel 76100.

‡Permanent address: Lawrence Livermore National Laboratory, Livermore, CA 94550.

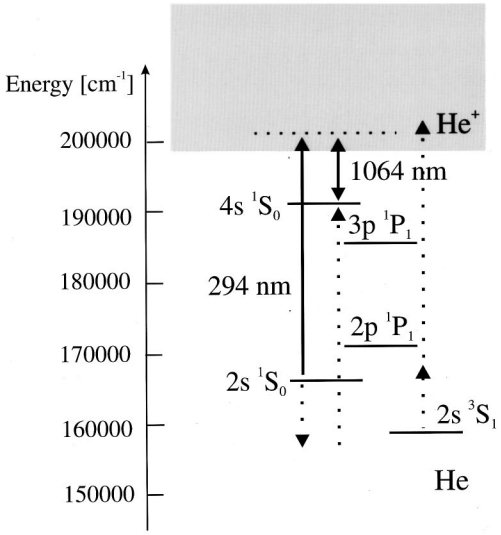

FIG. 1. Helium level scheme and the relevant couplings. The dressing laser ($\lambda_S = 1064$ nm) couples the excited state $4s\,^1S_0$ to the ionization continuum. The induced continuum structure is probed (at $\lambda_P = 294$ nm) through ionization of the $2s\,^1S_0$ state.

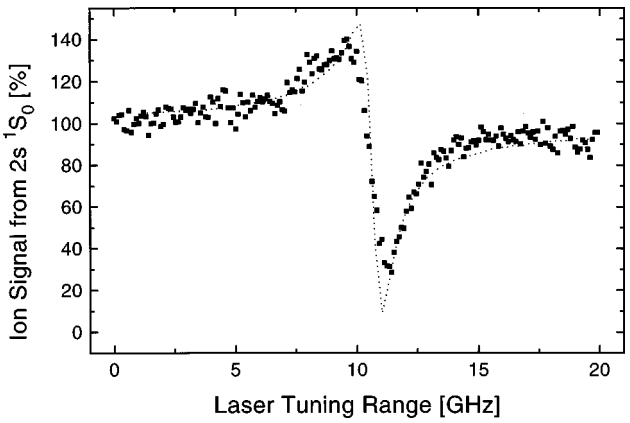

FIG. 2. Variations of the ionization cross section, probed with a weak probe pulse, the frequency of which is tuned across the two-photon resonance between the $2s\,^1S_0$ and $4s\,^1S_0$ states. The axis of the probe laser beam (diameter 0.5 mm) coincides with the axis of the dressing laser beam (diameter 3.5 mm). There is no time delay between the pulses. The laser intensities are $I_P = 4$ MW/cm^2 and $I_D = 75$ MW/cm^2. The experimental profile (dots) is in good agreement with the result from numerical studies (dotted line), which include averaging over fluctuating laser intensities and integrating over the spatial profile of the probe laser. With laser intensities stronger than those used for this figure, two-photon (IR plus UV) ionization of the $2s\,^3S_1$ state produces an additional background. This small contribution is determined from the difference of the ion signal with the dressing laser on and off, when the probe-laser frequency is tuned far off resonance from the LICS. For this figure such background was negligible.

(initially populated) metastable state $2s\,^1S_0$ to the ionization continuum.

To produce the probe pulse, laser light at 587 nm from a single-mode cw dye laser system is amplified in a pulsed dye amplifier, pumped by the second harmonic of an injection-seeded neodymium-doped yttrium aluminum garnet (Nd:YAG) laser. The wavelength of the cw radiation is measured to an accuracy of $\Delta\lambda/\lambda = 2\times10^{-6}$ in a Michelson-type wavemeter, using a He-Ne laser, stabilized on an iodine line, as a reference. The pulsed radiation is frequency-doubled in a BBO crystal, providing probe-laser pulses that have a pulse width $\Delta\tau = 2.3$ ns [half-width at $1/e$ of intensity $I(t)$]. The dressing radiation is obtained from the fundamental frequency of the Nd:YAG laser and has a width $\Delta\tau = 5.1$ ns. Our laser bandwidths (120 MHz for probe and 50 MHz for dressing laser) were within 10% of the Fourier limit, an essential requirement for observing deep narrow ionization-suppression features. A folded optical delay line is used to adjust the time delay between the probe and dressing pulses. In general, the strongest features are observed when the temporal overlap between the pulses is maximal, i.e., when the pulses coincide.

After passing through the optical setup, pulse energies of up to 250 mJ for the dressing laser and 1 mJ for the probe radiation are available for the experiment. The laser-beam diameters at the atomic beam position are 0.5 mm for the probe and 3.5 mm for the dressing laser, yielding intensities of up to 100 and 300 MW/cm^2, respectively. Thus, the variation of the dressing-laser intensity across the probe-laser profile is small.

LASER-INDUCED CONTINUUM STRUCTURE

When the probe laser is tuned across the two-photon resonance (between the states $2s\,^1S_0$ and $4s\,^1S_0$; see Fig. 1), we observe strong and spectrally narrow features in the ionization rate; see Fig. 2. These features can be regarded as a $4s\,^1S_0$ resonance embedded in the ionization continuum by the strong dressing laser (and probed by the weak probe laser).

The structure exhibits a typical asymmetric Beutler-Fano profile, in which the ionization rate is controlled by appropriately tuning the probe laser frequency, thereby selecting the region of enhanced or diminished ionization. At the minimum of the ionization profile the yield is reduced to less than 30% of its unperturbed value (in the absence of LICS). The figure also shows the result of numerical simulations, which are discussed in the following section.

We have found that the position of the profile minimum varies linearly with dressing pulse intensity (see Fig. 3). We discuss below the quantitative agreement of this result with our model computation.

THEORETICAL CALCULATIONS

Our calculations involve the formal adiabatic elimination of the continuum from the time-dependent Schrödinger equation [1], leading to a pair of coupled ordinary differential equations for the time dependence of the two bound-state amplitudes [6]. The atomic parameters needed in these equations are the bound-bound and bound-continuum dipole-transition moments. From these we construct the polarizabilities, photoionization cross-sections, and the Fano q parameter. The transition moments were evaluated using a model potential [23] for the valence electron states in the helium atom, in which an effective noninteger orbital angular

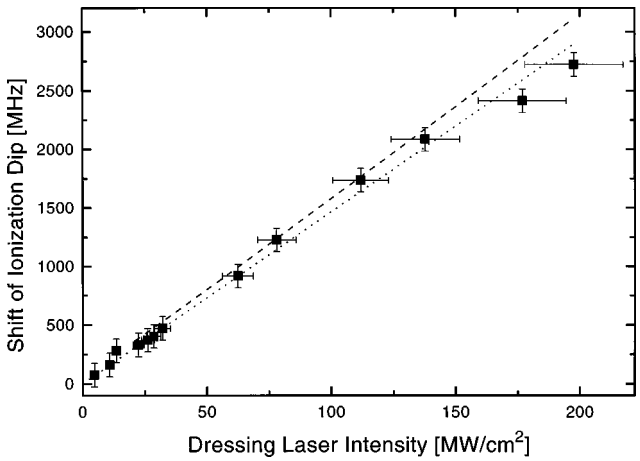

FIG. 3. Variation of the spectral position of the minimum of the laser-induced continuum structure with the dressing laser intensity. The dotted curve shows the calculated shifts of the ionization minimum. Very good agreement with the experimental data is found. The dashed curve shows the result of an analytical calculation for the Stark shift and power broadening for a short and weak probe pulse.

momentum quantum number, given as $\ell^* = \ell - n + (1/\sqrt{2|E_{n\ell}|})$, is defined from the ionization potential $E_{n\ell}$ (in atomic units) for orbital angular momentum ℓ and principal quantum number n.

This procedure allows us to obtain analytic expressions for the radial wave function and, in turn, for the dipole-transition moments. We have verified that wave functions constructed in this way are in good agreement with more accurate calculations of oscillator strengths, polarizabilities, and photoionization cross sections [24,25].

The calculated ionization rates from the states $2s\,^1S_0$ and $4s\,^1S_0$, produced by a probe laser of intensity I_P, are $\Gamma_{2s,P} = 13.4 I_P$, $\Gamma_{4s,P} = 1.9 I_P$. The dressing laser can only ionize the $4s\,^1S_0$ state; for an intensity I_D we obtain the ionization rate $\Gamma_{4s,D} = 73.7 I_D$. We express intensity in W/cm^2 and rates, and shifts below, in s^{-1}.

The calculated Fano q parameter for this LICS resonance is $q = 0.73$. The calculated Stark shifts produced by the probe pulse are $S_{2s,P} = 9.0 I_P$, $S_{4s,P} = 13.0 I_P$, and the calculated shifts produced by the dressing pulse are $S_{2s,D} = 70.0 I_D$, $S_{4s,D} = 142.0 I_D$.

The dynamic polarizability includes contributions from all other bound states and the ionization continuum. Because the coupling to bound states exceeds that to the continuum, the continuum gives only small contributions to these Stark shifts. The polarizability is greater at the frequency of the dressing laser than at the probe frequency, because the states that contribute to the former summation are closer to resonance. Because our dressing pulses are more intense than our probe pulses (and the polarizability is larger at the dressing frequency), the Stark shifts originate primarily with the dressing pulse.

The LICS, produced by an idealized cw laser (steady amplitude and single frequency), can differ substantially from the structure produced by a pulsed laser [16]. The time-dependent Stark shifts produce time-dependent detunings from both one- and two-photon resonance. Our simulation, as in previous work [6], not only includes pulse-shape effects but also averages the experimentally characterized intensity fluctuations of both lasers, and models the spatial beam profile of the probe laser. These several variations have pronounced effects on the predicted width and dip of the LICS profile.

It is appropriate to regard the action of the strong dressing pulse as embedding a $4s\,^1S_0$ resonance into the photoionization continuum. However, our modeling is not based upon this assumption; we treat both fields on an equal footing. It is the dressing and probe pulses together that produce a population-trapping state, superposing the $2s\,^1S_0$ and $4s\,^1S_0$ states.

DISCUSSION

The Fano parameter q of any resonance depends not only on the wave function of the resonance state and the associated continuum, but also on the particular observation channel [13]. In our photoionization observations the q is basically the ratio of a Raman polarizability to the product of two dipole transition moments into the continuum. In systems with $|q| > 1$ (such as the LICS with $q = 3.7$ as studied earlier [21,22]), the Raman-type transitions dominate. The ionization rate is enhanced, when tuning the probe laser across two-photon resonance, because Raman-type transitions open additional (multiphoton) ionization channels from the initial state to the ionization continuum. If $q = 0$, no Raman-type transitions are present, and no enhancement of ionization can be observed. The LICS revealed by scanning the probe frequency is then suppressed ionization.

In our experiment, for which q lies in the range $0 < |q| < 1$, the possibility occurs for both enhancement and substantial suppression of ionization. The dip in the ionization profile demonstrates population trapping. Therefore, observation of this feature depends critically on the coherence properties of the lasers.

The energies of states $2s\,^1S_0$ and $4s\,^1S_0$ both undergo dynamic Stark shifts. In our experiment the main contribution to these shifts comes from the strong dressing pulse. We find that the energies of both states shift upwards as the intensity of the dressing pulse increases.

The center position of the ionization profile is directly connected to the effective Stark shift of the two bound states. The position of the ionization minimum and maximum, with respect to this center, (i.e., the profile width) is also affected by pulse intensity (i.e., power broadening occurs). The position of the ionization minimum is measured with an accuracy on the order of the probe-laser bandwidth (120 MHz).

Our numerical calculations show that the positions of the characteristic features of the observed ionization structure (minimum, center, or maximum) depend nearly linearly on the peak intensity of the dressing laser. Figure 3 shows our experimental and theoretical values for the relative positions of the profile minimum for a range of dressing pulse intensities. Theory and experiment agree within expected errors.

CONCLUSIONS

We have observed strong spectrally narrow laser-induced continuum structure in the photoionization continuum of he-

lium. Our example shows both enhancement and pronounced ionization suppression (population trapping), associated with LICS, in an otherwise flat continuum. The narrow spectral width allows not only the use of this LICS as a spectroscopic tool, but also provides a basis for a stringent test of theory.

The observed positions of the LICS were found to be in very good agreement with calculations based on a simple model potential for the active electron. A more detailed set of observations and a discussion of analytical calculations of the LICS will be topics of future work, in which we will report in more detail the influence of intensity fluctuations, the spatial beam profiles, and the delay between probe and dressing pulse on the shape and bandwidth of LICS.

ACKNOWLEDGMENTS

The authors thank G. Torosyan and R. Unanyan, Institute for Physical Research of Armenian Academy of Sciences, Ashtarak, Armenia, for valuable help and discussions. M.S. and K.B. acknowledge support by the German Israeli Foundation. B.W.S. thanks the Alexander von Humboldt Stiftung for financial support; his work was supported in part under the auspices of the U.S. Department of Energy at Lawrence Livermore National Laboratory under Contract No. W-7405-Eng-48. L.Y. is grateful to the Deutsche Forschungsgemeinschaft for support of his visit to Kaiserslautern. This work received partial support by the EU network ''Laser Controlled Dynamics of Molecular Processes and Applications,'' Grant No. ERB-CH3-XCT-94-0603.

[1] P. L. Knight, M. A. Lauder, and B. J. Dalton, Phys. Rep. **190**, 1 (1990).
[2] O. Faucher, D. Charalambidis, C. Fotakis, J. Zhang, and P. Lambropolous, Phys. Rev. Lett. **70**, 3004 (1993).
[3] M. Shapiro, J. Chem. Phys. **101**, 3841 (1994).
[4] E. Frishman and M. Shapiro, Phys. Rev. A **54**, 3310 (1996).
[5] A. Vardi and M. Shapiro, J. Chem. Phys. **104**, 5490 (1996).
[6] L. P. Yatsenko, R. G. Unanyan, K. Bergmann, T. Halfmann, and B. W. Shore, Opt. Commun. **135**, 406 (1997).
[7] A. Vardi, D. Abrashkevich, E. Frishman, and M. Shapiro, J. Chem. Phys. **107**, 6166 (1997).
[8] T. Nakajima, M. Elk, J. Zhang, and P. Lambropolous, Phys. Rev. A **50**, R913 (1994).
[9] C. E. Carroll and F. T. Hioe, Phys. Rev. A **54**, 5147 (1996).
[10] E. Paspalakis, M. Protopapas, and P. L. Knight, Opt. Commun. **142**, 34 (1997).
[11] S. Schiemann, A. Kuhn, S. Steuerwald, and K. Bergmann, Phys. Rev. Lett. **71**, 3637 (1993); T. Halfmann and K. Bergmann, J. Chem. Phys. **104**, 7068 (1996).
[12] U. Fano, Phys. Rev. **124**, 1866 (1961).
[13] B. W. Shore, Rev. Mod. Phys. **39**, 429 (1967).
[14] K. Rzazewski and J. H. Eberly, Phys. Rev. Lett. **47**, 408 (1981).
[15] B.-N. Dai and P. Lambropoulos, Phys. Rev. A **36**, 5205 (1987).
[16] E. Paspalakis, M. Protopapas, and P. L. Knight, J. Phys. B **31**, 775 (1998).
[17] P. L. Knight, M. A. Lauder, P. M. Radmore, and B. J. Dalton, Acta Phys. Austriaca **56**, 103 (1984).
[18] E. Arimondo, Prog. Opt. **35**, 259 (1996).
[19] O. Faucher, Y. L. Shao, and D. Charalambidis, J. Phys. B **26**, L309 (1993); O. Faucher, Y. L. Shao, D. Charalambidis, and C. Fotakis, Phys. Rev. A **50**, 641 (1994); N. E. Karapanagioti, O. Faucher, Y. L. Shao, and D. Charalambidis, Phys. Rev. Lett. **74**, 2431 (1995).
[20] M. H. R. Hutchinson and K. M. M. Ness, Phys. Rev. Lett. **60**, 105 (1988); X. Tang, A. L'Huillier, P. Lambropoulos, M. H. R. Hutchinson, and K. M. M. Ness, *ibid.* **62**, 111 (1989); Y. L. Shao, D. Charalambidis, C. Fotakis, J. Zhang, and P. Lambropoulos, *ibid.* **67**, 3669 (1991); S. Cavalieri, F. S. Pavone, and M. Matera, *ibid.* **67**, 3673 (1991); S. Cavalieri, M. Matera, F. S. Pavone, J. Zhang, P. Lambropoulos, and T. Nakajima, Phys. Rev. A **47**, 4219 (1993); O. Faucher, Y. L. Shao, D. Charalambidis, and C. Fotakis, *ibid.* **50**, 641 (1994).
[21] S. Cavalieri, R. Eramo, and L. Fini, J. Phys. B **28**, 1793 (1995).
[22] R. Eramo, S. Cavalieri, L. Fini, M. Matera, and L. F. DiMauro, J. Phys. B **30**, 3789 (1997).
[23] N. L. Manakov and V. J. Ovsiannikov, J. Phys. B **10**, 569 (1977).
[24] M.-K. Chen, J. Phys. B **27**, 865 (1994).
[25] G. S. Hurst, M. G. Payne, S. D. Kramer, and J. P. Young, Rev. Mod. Phys. **51**, 767 (1979).